ORIGINAL PAPER

Synthesis, Physicochemical and Optical Characterization of Novel Fluorescing Complex: *o*-Phenylenediamine—Benzoin

Y. Dwivedi · Shiva Kant · S. B. Rai · R. N. Rai

Abstract The complex of *o*-phenylenediamine (*o*-PDA) and benzoin (BN) was synthesized adopting solid state reaction by mixing of their melt together followed by chilling. The phase diagram study shows the formation of a complex in 1:1 molar ratio with congruent melting point and two eutectics lying on either side of complex. The formation of complex was confirmed using the FTIR, NMR, mass spectroscopy, powder XRD and DSC studies. The optical properties of the parent component, their complex and few other compositions nearby the complex were studied using absorption and laser luminescence techniques. The significantly higher green/yellow emission was noted with newly synthesized complex as compared to that of their parents as well as other compositions of *o*- PDA and BN.

Keywords Solvent free synthesis · Eutectic · Fluorescence · Phase diagram · Green light emission · Charge transfer complex

PACS 87.64.k · 95.75.Fg · 42.62Fi · 78.00.oo · 78.47.Jc

Introduction

The potential application of organic materials for their versatile uses in fabrication of variety of devices such as nonlinear optical, electro-optic, semiconductors, lasers and superconductor devices has prompted researchers to explore the variety of novel organic materials of specific properties for specific applications [1–5]. Apart from the conventional synthesis of organic materials, the technique of molecular complexation has been developed as one of the designing tools in molecular crystal engineering [6] and this technique has been found capable to produce the promising optical organic materials as light emitting diode of different colors including white light [7]. However, very limited efforts have been made to synthesize molecular complexes based on interaction between two molecules adopting solid state reaction, and exploring the concept of phase diagram [8]. Studies of physicochemical properties of binary materials are very rare. Nevertheless, optical properties of some of the complexes have shown sensitivity to polarity, which is used as a probe to study the microenvironmental changes of the host as the polarity, influences the Stoke's shift of the complex.

Generally, in excited states the separation of charges is different to that of charge distribution of complex in their ground state that is one of the root causes for various transformations of chemical and biological complex [9–12]. Further electron donor-acceptor molecules have been found ideal for charge transfer process [13]. These complexes are useful for the study of solvation dynamics [14], nonlinear optical properties [15], in laser applications [16] and have also been used as fluorescence probes [17, 18].

Phenylenediamine (PDA) is found in ortho, meta and para isomeric forms and is used in syntheses of commercial hair dyes, polyamides, maleimides and agricultural pesticides. Particularly, polymerised *o*-phenylenediamine (*o*-PDA) is used for various applications such as for immobilization of bioactive materials, electrocatalysis,

Y. Dwivedi · S. B. Rai
Laser and Spectroscopy Laboratory, Physics Department,
Banaras Hindu University,
Varanasi, India 221005

S. Kant · R. N. Rai (✉)
Department of Chemistry, Banaras Hindu University,
Varanasi, India 221005
e-mail: rn_rai@yahoo.co.in

corrosion inhibition, and as electrochromic materials [19]. On the other hand benzoin (BN) is employed for photocatalyst, chelating and other applications [20]. The *o*-PDA has two amino groups and BN has a carbonyl group therefore the probability of interaction between electron donor and electron acceptor group are very high. The work started with thought that the complex formed would be interesting for various applications. Thus, the *o*-PDA and BN have chosen for the investigations in detail.

In this paper, detail of investigations concerning the identification of specific composition of molecular complex via establishing phase diagram between *o*-PDA and BN are reported. For the determination of suitable composition that forms the complex, the phase diagram has been studied in detailed however for the synthesis of material, solid state reactions has been employed. For the confirmation of complex formation, powder XRD, DSC, FTIR, NMR and mass spectroscopy techniques are used. We also report the structural, thermal and optical properties of the newly synthesized complex and for comparison the properties have been compared with the parent components.

Experimental Section

Complex Synthesis and Experimental

The starting material *o*-phenylenediamine (S.D. fine chemicals, India) was purified by zone refining technique, while benzoin compound (Sigma Aldrich) was purified by crystallization from CCl_4. The purity of each compound was checked by comparing their melting points. The complex of the BN and *o*-PDA has been synthesized by the application of solid state reaction under chilling and homogenization process, in which parent components were taken in various molar compositions. The compositions were melted slightly above (4 °C) the melting temperature of the parents. The molten mixture of the both parents was homogenized and chilled in ice cooled water (5 °C). The homogenization and chilling process were repeated up to four times for the completion of reaction.

Infrared spectra of parent components and their complex were measured in transmittance mode in the region 400–4000 cm^{-1} by dispersing and palletizing in KBr. The resolution of FT-IR spectrometer [Perkin Elmer RX-1] was 2.0 cm^{-1}. Baseline corrections were introduced whenever needed. The mass spectrum of the complex was recorded on Micromass Quattro II system, Micromass, UK while NMR spectra were recorded on FTNMR-JOEL AL300 system. The Differential Thermal Calorimetry (DSC) curve has been recorded using Mettler TA 4,000 machine under N_2 gas

atmosphere. The UV absorption spectra of the parent molecules and their complex were recorded in solution of EtOH solvent, using JASCO V-670 absorption spectrophotometer in the range 200–2,300 nm. The fluorescence measurements were carried out using forth (266 nm) and the third (355 nm) harmonics of Nd:YAG laser (Spitlight 600, Innolas, Germany) as an excitation source. Laser beam was focused onto the sample using convex lens (focal length ~8 cm) and the spot size at sample was ~100 μm. To detect the dispersed luminescence, emission from sample was collected in perpendicular direction to that of on the slit of computer controlled Trix monochromator iHR320 equipped with grating blazed at 500 nm and PMT (model 1424 M). The resolution of monochromator was ~0.2 nm. All measurements were taken at identical conditions and at ambient temperature (26±2 °C).

Phase-diagram

The phase diagram of *o*-PDA and BN system was studied using thaw melt method and the phase diagram was established in melting temperature vs composition [21]. In this method, the mixture of the two compounds covering entire range of compositions were prepared and their melts were homogenized together by continuous shaking, followed by chilling in ice cold water. The melting temperature of each composition was recorded using a melting point apparatus attached with a precision thermometer (±0.5 °C).

Results and Discussions

Thermal Analysis

The phase diagram of *o*-PDA and BN has been established between freshly prepared entire range of compositions of two compounds and their respective melting points were determined and the diagram has been depicted in Fig. 1. The diagram shows the formation of a molecular complex (A) with congruent melting point having two eutectics E_1 and E_2 on either side. The composition mole fraction of *o*-PDA in E_1, E_2, and the complex are 0.35, 0.80 and 0.50, respectively. It is evident from the figure that the melting point of BN decreases with the addition of *o*-PDA, and attains a minimum value at the first eutectic point E_1. Further addition of *o*-PDA causes the melting point to rise and attain a maximum at A. The diagram shows that the addition compound (A) melts congruently i.e. the compositions of liquid and the solid phases are identical. Onwards, addition of *o*-PDA beyond causes a decrease in melting temperature and attains a minimum at second eutectic point E_2. At eutectic temperatures, the two solid
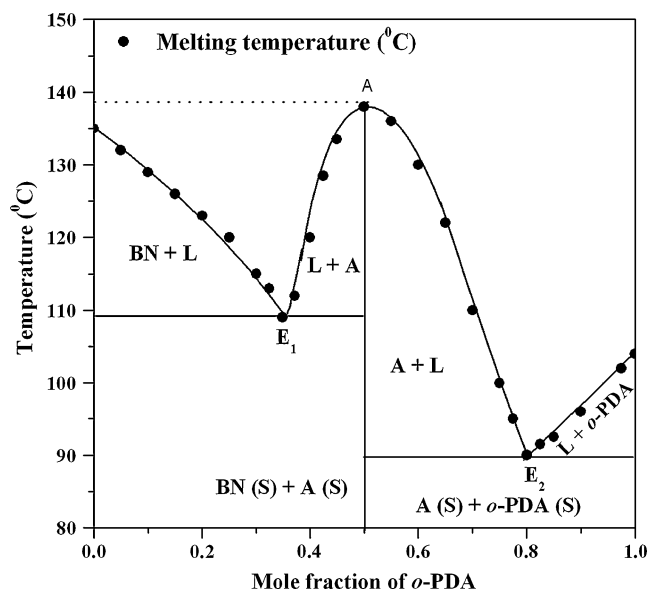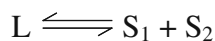
Fig. 1 Phase diagram of *o*-PDA and BN system, established between different compositions of *o*-PDA and BN and their respective melting point

phases and a liquid phase are in equilibrium. The eutectic reactions may be, schematically, represented as:

$$L \rightleftharpoons S_1 + S_2$$

The melting temperatures of E_1, E_2 and A were found to be 118, 90, and 138 °C, respectively. It was also noted that the composition of complex as well as immediate adjacent compositions to the complex solidify late even in ice cold water. This observation of late solidification has reflected in XRD where the crystallinity of the complex was found to be poor.

The thermal properties and stability of BN, *o*-PDA and their complex have been studied and their DSC curves are depicted in Fig. 2. The heat of fusion values of BN, *o*-PDA and complex are found to be 40.3, 26.3 and 11.8 kJ mol^{-1} respectively. The DSC curve of the complex shows a single broad peak and the peaks corresponding to melting temperatures of pure BN and *o*-PDA compound are not found in the curve. The melting point of the complex is substantially higher than that of the parent compounds. The higher melting point and existence of a single peak for the complex indicates that the complex formed is of single and pure nature, which could be considered as a new species.

Structural Analysis

(a) NMR and mass spectroscopy

The NMR (^{1}H and ^{13}C) spectrum of BN, *o*-PDA and the complex has been recorded in CDCl$_3$ solvent. In ^{1}H

spectrum of complex, the peak for NH$_2$ proton of *o*-PDA (3.37 ppm) is absent. Also the peak for carbonyl carbon of benzoin (198.88 ppm) is disappeared in ^{13}C of complex. Apart from these changes, a new signal peak is observed at 157.62 ppm, which could be due to the azomethine carbon (C=N), this finding indicates the formation of complex. The detail peak analysis is as:

2, 3-Diphenyl-1, 2-dihydro-quinoxaline ^{1}H NMR (CDC^{13}, 300MHz) [δ 4.42 (s, 1H, NH), δ 5.68 (s, 1H, CH), δ 6.51-6.48 (d, 2H, ArH), δ 6.82-7.77 (m, 2H, ArH),δ 7.03-6.98 (m, 2H, ArH), δ 7.50-7.35 (m, 6H, ArH), δ 7.93-7.90 (m, 2H, ArH)], ^{13}C NMR (300 MHz, CDC^{13}) [δ 157.62, 140.64, 137.02, 134.93, 133.03, 130.17, 129.14, 128.64, 128.37, 128.23, 128.06, 127.07, 126.55, 118.91, 113.73, 54.67].

The mass spectrum of the complex shows the molecular ion peak (m/z) corresponding to its relative abundance which are 285 (M+1, 100), 286 (M+2, 24), 283 (M-1, 30), 208 (26), 207 (14), 167 (10), 388(7). The fragmentation of the parents lead to the 2, 3-Diphenyl-1, 2-dihydro-quinoxaline complex as the main fragmentation path is shown in Fig. 3. The mass spectra provided further vital clue in elucidation of the structure of the complex formation. The most probable structure and the reaction mechanism that could be assigned using NMR and mass spectroscopy are shown in Fig. 3.

(b) Powder XRD

In order to understand the nature of the complex whether parent components are associated to form a new complex or forming a mechanical mixture, X-ray powder diffraction patterns of the complex and the parent components, *o*-PDA
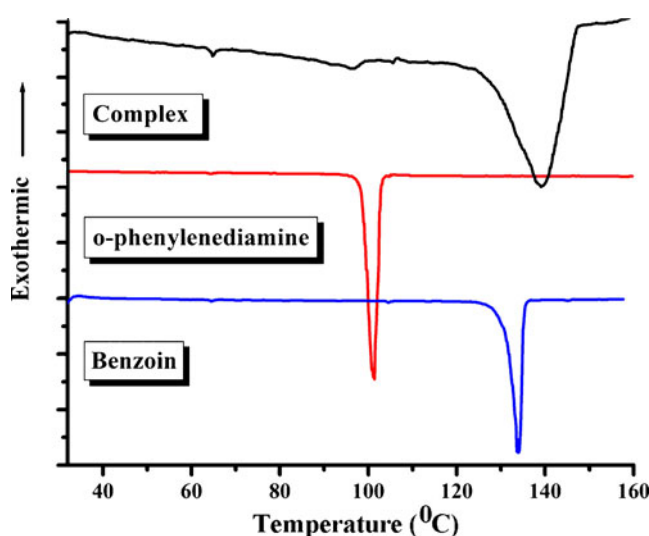

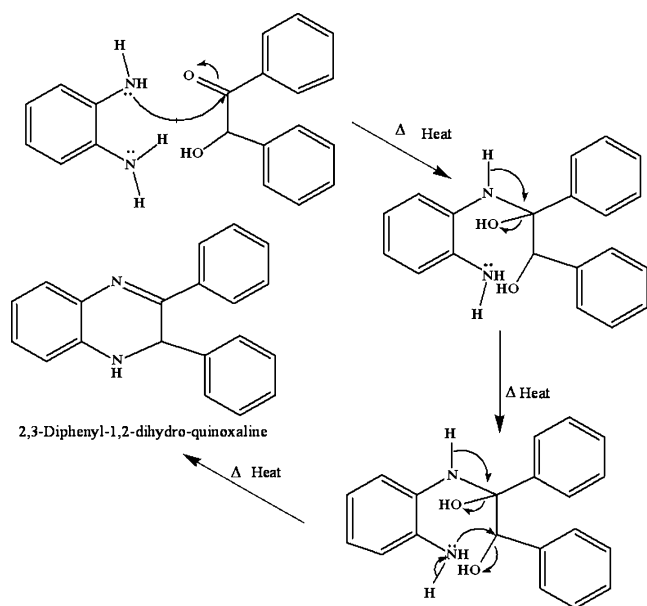**Fig. 2** Differential scanning calorimetric curve of the BN, *o*-PDA and their complex

Fig. 3 The reaction mechanism for the complex formation

2,3-Diphenyl-1,2-dihydro-quinoxaline

and BN, were recorded and depicted in Fig. 4. In the powder XRD pattern of benzoin, the bragg peaks has been indexed to the monoclinic cell (a=18.69, b=5.774, c=10.41Å, and β=105.55°) and compared using JCPDS data card 30-1542. The powder X-Ray diffraction pattern of o-PDA has also shown the monophase crystalline structure as the reported values in JCPDS data file 04-0238.

In XRD pattern of the complex several new peaks were observed which belongs to neither of the parent components. This study infers the formation of new molecular complex of entirely different nature. This finding supports the phase diagram study where the complex formation has inferred.
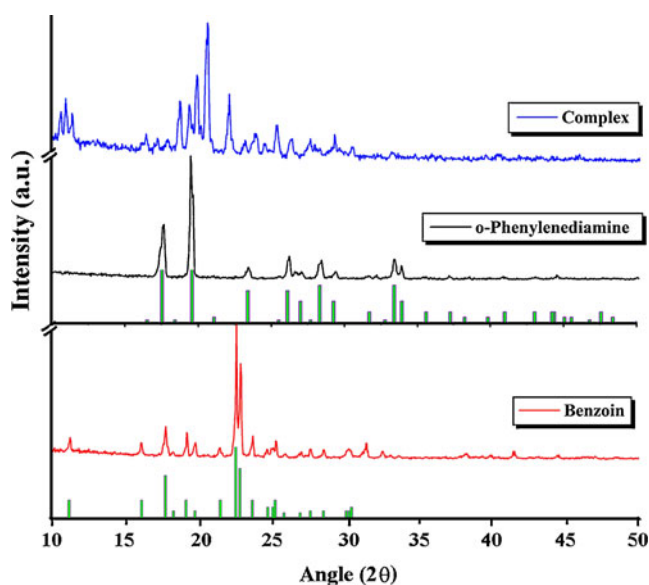

Fig. 4 XRD patterns of BN, o-PDA and their complex

Spectroscopic Properties

Absorption Analysis

(i) UV-Visible absorption

The optical absorption spectra of BN, o-PDA and the complex have been recorded in the range of UV-Vis. region (200–900 nm) in EtOH solution and have shown in Fig. 5. The UV/Vis. Absorption spectrum of BN shows three peaks at 217 nm, 238 nm and 258 nm which ascribed to the $\pi\rightarrow\pi^*$ transitions due to the presence of the phenyl ketone group (Ar-C=O), in which the carbonyl group is conjugated with the benzene ring. The bands observed in absorption spectrum of o-PDA are found in agreement as reported by Manoharan et al. [22]. The bands at 220 and 238 nm are attributed due to the $\pi\rightarrow\pi^*$ transition while a strong band at 295 nm appears due to the amino group [23].

The observed red shift in complex is related to the structural changes due to the interaction of o-PDA and BN in EtOH. It is considered that when o-PDA interact with the BN, water molecule is being removed and the nitrogen atom of amino group of o-PDA is attached with the C atom and getting converted to C=NR'NH$_2$, consequently the electron density of the C=O bond reduces, which causes a red shift in absorption [24, 25]. This finding is in accordance with the fact that de-protonation of amino group gives red shifted absorption maxima [26–29]. Another interesting observation is that the peak corresponding to the amino group at 295 nm in o-PDA reduces significantly in complex which indicates the reduction of the number of amino groups (–NH$_2$) in the complex.

In BN absorption spectrum, two weak bands appear at 285 and 326 nm which ascribed as n$\rightarrow\pi^*$ transitions. These bands become intense and broad in complex and suffer a
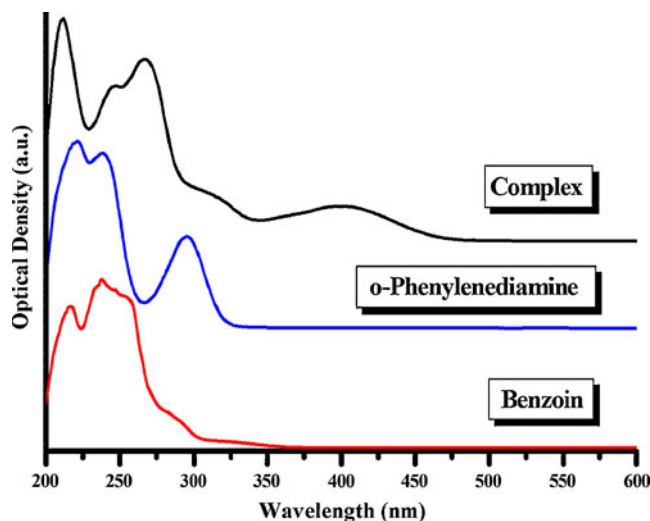

Fig. 5 UV/Vis absorption spectra of BN, o-PDA and complex in EtOH solution

small bathocromic shift in solvents and this shift differs with polarity of solvent. Typically, in a charge-transfer transitions, an increase in the polarity of the medium leads to a Stokes shift of the absorption maximum. The detail of bathochromic shift is discussed in luminescence section of the manuscript.

(ii)   IR absorption

FT-IR absorption spectra of BN, *o*-PDA and their complex have been recorded in the range of 400–4000 cm^{-1} in solution (EtOH) as well as in solid (Fig. 6). However to record the solid IR absorption samples were dispersed in KBr and palletized. The validity of the peaks assigned for the three compounds have also been verified by theoretical calculation, which are carried out using Density Functional Theory (DFT) with B3LYP/6-311G* basis set. The recorded FT-IR spectrum of *o*-PDA was found to be in good agreement with the spectrum as reported by Ohmasa *et al.* [30]. In the FT-IR spectrum of the solid *o*-PDA, the bands at 3386 cm^{-1} and 3364 cm^{-1} are due to –NH$_2$ group, which are the characteristic symmetric and asymmetric -N-H stretching vibrations. The broad peaks around 3,188 and 3,289 cm^{-1} can be assigned for the N–H stretching vibration of the –NH$_2$ group. On the other hand in solution these N-H bands are buried in the broad –OH vibration peak due to the presence of EtOH. Particularly, in case of solid the N-H stretching modes are usually observed sharper than O-H stretching modes. The band observed in the 2,800–3,100 cm^{-1} region is the characteristic ν_{CH} bands of the aromatic ring vibrations.

Bands observed at 1630.2 and 1633.4 cm^{-1} are due to the N-H wagging in solution and solid, respectively. The bands observed between ~1,590 and ~1,620 cm^{-1} are ascribed to C=C stretching mode. The intense band at
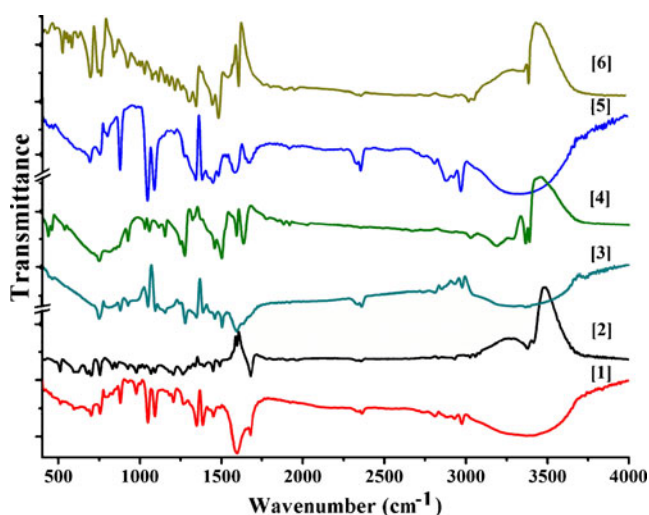
1,482 cm^{-1} is associated with the vibrations of the C-N-H group mixed with C-C stretching and CH bending. A strong band observed at 1,343 cm^{-1} results from the interaction between the N-H and C-H bending and C-N stretching vibrations. The band observed between 1,112 and 1,214 cm^{-1} is attributed to CH bending vibrations. The peaks at 1,243 and 1,247 cm^{-1} are associated with the C–N stretching in the solution and solid samples, respectively.

Infra-red absorption spectrum of BN was also found in agreement with data reported earlier [31] and a broad band of -OH vibration at 3,382 cm^{-1} in solution was observed. However in solid, two bands at 3376.6 and 3414.7 cm^{-1} with comparatively weak intensity are observed and they due to –OH vibrations. The additional broadening observed in solution was expected due to the strong interaction of BN with host (EtOH). An intense and well-defined peak observed at 1,680 cm^{-1} is due to the stretching vibration of carbonyl group. The peak at 1,205 cm^{-1} is due to the C-O vibrations in solid and solution. The FT-IR study of complex has inferred important information about the structural changes occurred due to interaction between BN and *o*-PDA. The spectrum shows that there are few bands which are either shifted or invisible in comparison to their parent molecules, and also some peaks of BN and *o*-PDA are present, with a change in intensity, in the spectrum of complex. Among these bands, the strong absorption band due to carbonyl (~1,680 cm^{-1}) of BN is found to be absent and a new sharp band corresponding to C=N group (~1,605 cm^{-1}) is appears in solid [15]. These drastic changes indicate the structural changes of the complex to that of parent components.

Fluorescence Analysis

Fluorescence spectra of BN, *o*-PDA and their complex have been recorded under 266 and 355 nm excitations and they are discussed separately as follows:

(i)   Excitation with 266 nm

Fluorescence spectrum of BN, *o*-PDA and their complex recorded under 266 nm laser excitations and the spectra thus obtained were shown in Fig. 7. Solid *o*-PDA emits strong (green) emission at 538 nm radiation (FWHM ~50 nm) while the BN give very weak emission at 500 nm which is difficult to record. When the BN and *o*-PDA in 1:1 ratio are mixed in EtOH solvent, it gives strong asymmetrical yellow band (574.83 nm) with large Stock shift (~308 nm). It was noted that the emission of complex was markedly red shifted (~35 nm) compared to pure *o*-PDA emission. An interesting observation is that the emission of complex enhances in both, 2.5 times in solid and 3.2 times in solution as compared to maximum emission recorded with *o*-PDA in solid and solution form.
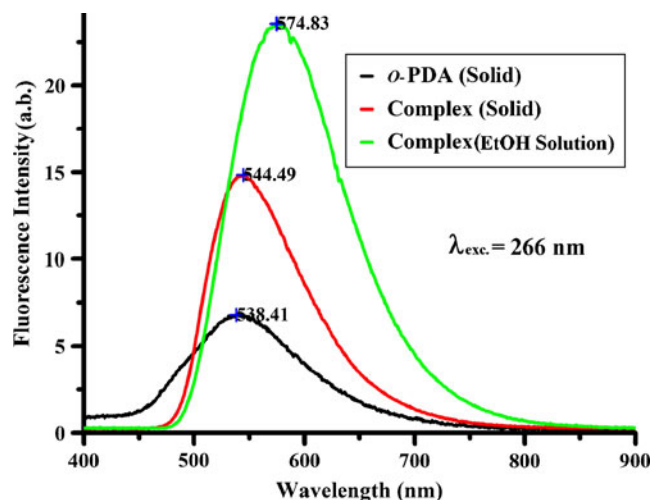

Fig. 6 FT-IR spectrum of BN (*1, 2*), *o*-PDA (*3, 4*) and Complex (*5, 6*) in EtOH solution and solid, respectively

Fig. 7 Fluorescence spectrum of BN, o-PDA and their complex formed in EtOH solution and solid under 266 nm photon excitation

To get the maximum fluorescence intensity, the concentration of binary (BN and o-PDA) was optimized and 1:1 ratio of BN and o-PDA emission was found to be maximum.

(ii) 355 nm excitation

On excitation with 355 nm laser photons, o-PDA and BN yield weak band at 519 and 493 nm respectively, due to their small absorption coefficient in 355 nm region. However fluorescence spectrum of the complex reveals a drastic enhancement (ten times) in emission intensity compare to 266 nm excitation (Fig. 8). The enhancement in the emission intensity of complex is larger in solution compared to solid.

The emission of the complex is much higher with 355 nm excitation compared to the emission observed with 266 nm. A large red shift of ~30 nm is noted in solution on 355 nm excitation compared to solid similar to the emission pattern observed in 266 nm excitation. The solvatochromic properties of the complex are correlated with electronic spectra of complex taking in different solvent of different polarities viz. hexane, carbon tetrachloride, ethanol, tetra hydofluoron, acetone, acetonitrile, Dimethylformamide, and water. Table 1 lists the wavelength of maximum absorption and fluorescence along with the Stocks shifts of complex in different polar solvents. It was noted that with the increase of polarity of solvent the emission band significantly shifted towards red. The observed large shifting can be explained as: when an electron donating group (amino group), and an electron accepting group (carbonyl group) combine with each other directly or through a bridge of conjugated double bonds, the migration of electrons are possible from former to the latter, as a result of this the complex gives rise a special absorption band totally different from the parent components. By analogy
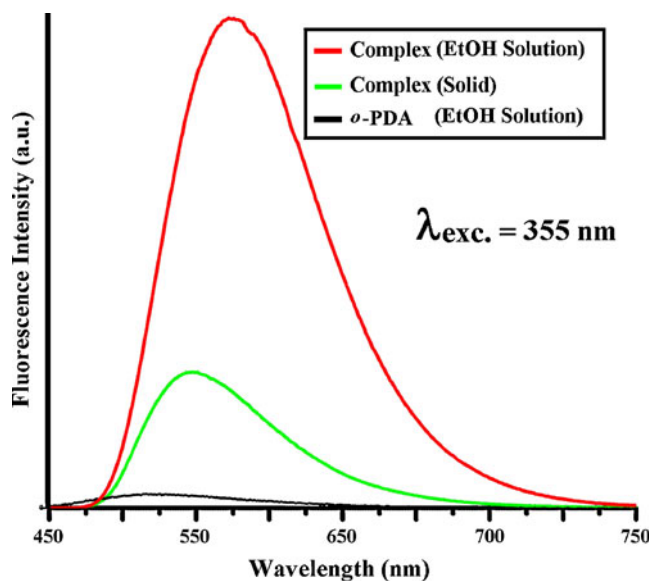
with the case of molecular compounds (considering a single entities), it may be called intramolecular charge transfer absorption bands.

In fact, Nagakura et al. showed in an earlier report that strong absorption bands observed in a number of molecules containing the nitro or carbonyl group can be interpreted as intramolecular charge-transfer absorption bands [32–34]. This improves extinction corresponding to 355 nm consequently enhanced fluorescence intensity. For comparison a visualized emissions of parents and the complex under 355 nm excitations at uniform conditions such as concentrations and laser power etc. is depicted in Fig. 9.

Charge transfer fluorescence transitions are sensitive to the polarity and the dielectric constant of the solvent. Variation in wavelength of maximum absorption and fluorescence have been plotted in terms of Lippert-Mataga solvent polarity parameter Δf, which is the function of

Fig. 8 Fluorescence spectrum of o-PDA and their complex in EtOH solution and solid under 355 nm photon excitation

Table 1 Wavelength of maximum UV-Vis absorption and fluorescence and corresponding Stoke's Shift of complex in different polar solvents

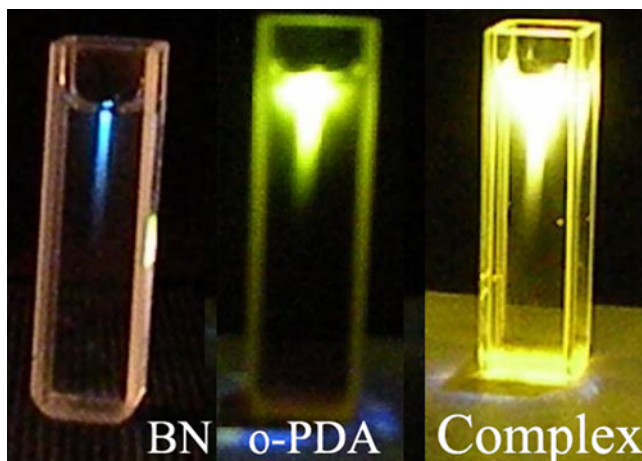| Solvent	Absorption λ_{max} (nm)	Fluorescence λ_{max} (nm)	Stoke's shift $\Delta \nu$ (cm^{-1})
Carbon Tetrachloride	398	504	6676
Tetrahydrofluron	400	544	6618
Acetone	398	532	6329
Ethenol	402	573	7424
Acetonitrile	394	547	7099
Dimethylformamide	404.8	553	6620
Water	407	552	6454

Fig. 9 A visualized observation for comparison of emissions between the parents BN, *o*-PDA and their complex under 355 nm excitations

static dielectric constant ε and the refractive index of the solvent and are related as [35, 36]:

$$\Delta f = [(\varepsilon - 1)/(2\varepsilon + 1)] - [(n^2 - 1)/(2n^2 + 1)] \quad (1)$$

Both the spectra show the linear variation with the polarity of the solvents.

However the fluorescence spectra are observed to be highly sensitive to the solvent polarity, compared to the absorption spectrum as the slope of the fluorescence plot is (slope=0.207) higher than the slop of absorption plot (slope=0.0145) Fig. 10. This large difference suggests that the excited state of the complex is significantly polar compare to the ground state.

The red shift of emission peaks with change of polarity of solvents are predominant than the shifts in absorption
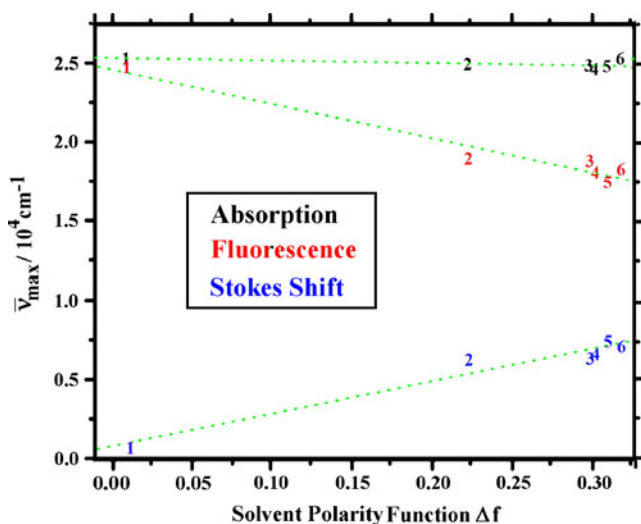

Fig. 10 Lippert-Mataga plots of absorption; fluorescence and Stock's shift against the solvent polarity function (Δf) of complex in (*1*) CCl₄, (*2*) THF, (*3*) Acetone, (*4*) DMF, (*5*) Ethenol and (*6*) Acetonitrile solvents

peaks. This indicates that Δμ is positive i.e. the dipole moment of the complex studied here increases on excitation. Also, the large magnitude of Stokes shift indicates that the excited state geometry is different from that of the ground state geometry. It is a general observation that an increase in the Stoke's shifts with the polarity shows the increment in the dipole moment. The full width at half maximum (FWHM) of absorption band and fluorescence bands in polar solvent is broader and it also varies linearly with their polarity.

For the molecules in which the fluorescence and the absorption bands appears with the same excited and ground states, the Stoke shift $\left(\Delta v = v_{abs}^{max} - v_{flu}^{max} \right)$ is expected to follow a linear relation with Δf [37]:

$$\Delta v = \Delta v_0 + 2\left(\mu_e - \mu_g \right)^2 / hca_0^3 \quad (2)$$

where μ_e = excited state dipole moment, μ_g = ground state dipole moment, h = plank constant, c = light velocity, a_0 = Onsager cavity radius of interaction.

The values of the Onsagar cavity radii (a_o) were calculated from the molar volume of molecules using the Suppan's equation [38]:

$$a_o = (3M/4\pi\delta N)^{1/3} \quad (3)$$

where δ is the density of the solute molecule, *M* is the molecular weight of solute and *N* is the Avogadro number.

The Lippert-Mataga plot for Stokes shift clearly demonstrates the solvent polarity sensitive behavior of the complex. A large Stokes shifted emission is observed in different solvents, suggesting the higher charge transfer in the excited state than in the ground state. From the slope of the plot, the value μ_e of complex is estimated and found to be ~7.0625 D keeping μ_g=2.6763 D (value obtained from quantum chemical calculation method) and a_0=22Å. Such a high μ_e value speculated to the S₁ state of the complex shows strong intramolecular charge transfer (ICT) character. By separating μ_e in protic and aprotic solvents, it was noted that the excited state dipole moment in protic solvents (μ_e~5.52 D) is higher than in aprotic solvents (μ_e~5.41 D). This indicates the specific hydrogen bonding interaction between solute-solvent which might be causing an enhancement in the ICT character for the complex. Similar hydrogen bonding effects on the charge transfer characteristic of other probe molecules have also been found in literature [39].

Conclusion

A novel complex of *o*-phenylenediamine and benzoin has been synthesized adopting solid state reaction by mixing their melt together followed by chilling. The phase diagram

study shows the formation of a complex with congruent melting point and two eutectics lying on either side of complex. The complex composition, o-PDA and BN, has been determined by establishing the phase diagram in the entire range of compositions of two compounds. The complex formation was confirmed by studying the FTIR, NMR, mass spectroscopy, powder XRD and DSC techniques. The optical properties of the individual and the complex have been evaluated using UV-Vis absorption and laser fluorescence techniques. The complex was noted to give intense green/yellow emission as compared to their parents. It was noted that the emission is stronger in complex composition (1:1) than other compositions of BN and o-PDA. Absorption and the laser fluorescence of the complex show its higher sensitivity to the polarity of the solvents. Spectral shift in absorption/emission band and enhancement in emission intensity is proposed due to the intramolecular charge transfer in complex.

References

1. Thompson J, Blyth RIR, Mazzeo M, Anni M, Gigli G, Cingolani R (2001) White light emission from blends of blue-emitting organic molecules: a general route to the white organic light-emitting diode. Appl Phys Lett 79:560–562

2. Pereverzev YV, Gunnerson KN, Prezhdo OV, Sullivan PA, Liao Y, Olbricht BC, Akelaitis AJP, Jen AKY, Dalton LR (2008) Guest–Host cooperativity in organic materials greatly enhances the nonlinear optical response. J Phys Chem C 112:4355–4363

3. Inokuchi H (2006) The discovery of organic semiconductors. Its light and shadow. Org Electron 7:62–76

4. Inokuchi H (1989) Organic semiconductors, conductors and superconductors. Int Rev Phys Chem 8:95–124

5. Dwivedi Y, Rai SB, Thakur SN (2008) Optical properties of Rh 6G dye in liquid and solid polymer. Spectrochim Acta A 69:789–793

6. Muthuraman M, Masse R, Nicoud JF, Desiraju GR (2001) Molecular complexation as a design tool in the crystal engineering of non-centrosymmetric structures. Ideal orientation of chromophores linked by O−H···O and C−H···O hydrogen bonds for nonlinear optics. Chem Mater 13:1473–1479

7. Jou JH, Sun MC, Chou HH, Li CH (2006) Efficient pure-white organic light-emitting diodes with a solution-processed, binary-host employing single emission layer. Appl Phys Lett 88:141101–141103

8. Rothenberg G, Downie AP, Raston CL, Scott JL (2001) Understanding solid/solid organic reactions. J Am Chem Soc 123:8701–8708

9. Singh AK, Kanvah S (2000) Effect of microheterogeneous media on the fluorescence and fluorescence probe properties of donor–acceptor diarylbutadienes. New J Chem 24:639–646

10. Diner BA, Babcock GT (1996) Structure, dynamics, and energy conversion efficiency in photosystem II. In: Ort DR, Yocum CF (eds) Kluwer academic Publishers, Netherlands

11. Bard AJ, Fox MA (1995) Artificial photosynthesis: solar splitting of water to hydrogen and oxygen. Acc Chem Res 28:141–145

12. Meyer TJ (1989) Chemical approaches to artificial photosynthesis. Acc Chem Res 22:163–170

13. Wasielewski MR (1992) Photoinduced electron transfer in supramolecular systems for artificial photosynthesis. Chem Rev 92:435–461

14. Nandi N, Bhattacharyya K, Bagchi B (2000) Dielectric relaxation and solvation dynamics of water in ccomplex chemical and biological systems. Chem Rev 100:2013–2046

15. Chemla DS, Zyss J (1987) Nonlinear optical properties of organic molecules and crystals. Academic, New York

16. Maeda M (1984) Laser dyes. Academic, New York

17. Singh AK, Darshi M (2004) A fluorescence study of (4-{(1E, 3E)-4-[4-(dimethylamino)phenyl]buta-1, 3-dienyl}phenyl)methanol and its bioconjugates with bovine and human serum albumins. New J Chem 28:120–126

18. Saroja G, Ramachandram B, Saha S, Samanta A (1999) The fluorescence response of a structurally modified 4-aminophthalimide derivative covalently attached to a fatty acid in homogeneous and micellar environments. J Phys Chem B 103:2906–2911

19. Tu X, Xie Q, Wang M, Zhang Y, Yao S (2005) A piezoelectric spectro- electrochemical study on the structural interconversion for poly(o-phenylenediamine) between its ladder structure with phenazine units and polyaniline-like chains. Chin Sci Bull 50:1598–1604

20. Raju NA, Rao GG (1955) Benzoin as a fluorescent reagent for the detection of germanium. Nature 175:167–167

21. Rai US, Rai RN (1999) Physical chemistry of organic eutectic and monotectic: hexamethylbenzene−succinonitrile system, *Chem. Mater* 11:3031–3036

22. Manoharan R, Dogra SK (1987) Spectral characteristics of phenylenediamines and their various protonated species. Bull Chem Soc Jpn 60:4409–4415

23. Li XG, Wang HY, Huang MR (2007) Synthesis, film-forming, and electronic properties of o-phenylenediamine copolymers displaying: an uncommon tricolor. Macromolecules 40:1489–1496

24. Koppel IA, Taft RW, Anvia F, Zhu SZ, Hu LQ, Sung KS, DesMarteau DD, Yagupolskii LM, Yagupolskii YL, Ignat'ev NV, Kondratenko NV, Volkonskii AY, Vlasov VM, Notario R, Maria PC (1994) The gas-phase acidities of very strong neutral bronsted acids. J Am Chem Soc 116:3047

25. Koppel IA, Koppel J, Leito I, Koppel I, Mishima M, Yagupolskii LM (2001) The enormous acidifying effect of the supersubstituent =NSO$_2$CF$_3$on the acidity of derivatives of benzenesulfonamide and toluene-p-sulfonamide in the gas phase and in dimethyl sulfoxide. J Chem Soc, Perkin Trans 2:229–232

26. Sinha HK, Dogra SK (1989) Electronic Spectra of benzimidazofecarboxylic acids:effect of solvent and acid concentration. Spectrochim Acta A 45:1289–1295

27. Dey JK, Dogra SK (1991) Solvatochromism and prototropism of 2-(3′-hydroxyphenyl)benzoxazole and 2-(4′-hydroxyphenyl)benzoxazole in the excited singlet state. J Photochem Photobiol A 59:307–321

28. Rajendiran N, Swaminathan M (1996) Spectral characteristics of 4-aminodiphenyl ether in different solvents and at various pH values. J Photochem Photobiol A 93:103–108

29. Rajendiran N, Swaminathan M (1995) Solvatochromism and prototropism of diaminodiphenyl sulphones and 2-aminodiphenyl sulphone: a comparative study by electronic spectra. J Photochem Photobiol A 90:109–116

30. Ohmasa M, Kinoshita M, Akamatu H (1971) Two types of complexes of o-Phenylenediamine with tetracyanoquinodimethane. Bull Chem Soc Jpn 44:3296–3298

31. Pawelka Z, Kryachko ES, Huyskens TZ (2003) Theoretical and experimental study of the conformational and vibrational properties of benzoin. Chem Phys 287:143–153

32. Nagakura S, Tanaka J (1954) The relation between energy levels of substituent groups and electron migration effects in some monosubstituted benzenes. J Chem Phys 22:236–240

33. Nagakura S (1955) Intramolecular charge transfer spectra observed with some compound containing the nitro or the carbonyl group. J Chem Phys 23:1441–1445

34. Tanaka J, Nagakura S (1956) Appearance of two intramolecular charge transfer absorptions observed with some disubstituted benzenes. J Chem Phys 24:1274–1275

35. Do J, Huh J, Kim E (2009) Solvatochromic fluorescence of piperazine-modified bipyridazines for an organic solvent-sensitive film. Langmuir 25:9405–9412

36. Mataga N, Kaifu Y, Koizumi M (1956) Solvent effects upon fluorescence spectra and the dipole moments of excited molecules. Bull Chem Soc Jpn 29:465–470

37. Ghosh HN, Pal H, Sapre AV, Mittal JP (1993) Charge recombination reactions in photoexcited fullerene C60-amine complexes studied by picosecond pump probe spectroscopy. J Am Chem Soc 115:11722–11717

38. Suppan P (1983) Excited-state dipole moments from absorption/fluorescence solvatochromic ratios. Chem Phys Lett 94:272–275

39. Aich S, Raha C, Basu S (1997) Characterization of the triplet charge-transfer state of 4-amino-N-methylphthalimide in aprotic and protic media by laser flash photolysis. J Chem Soc Faraday Trans 93:2991–2996